7-2002

Non-Dipolar Electron Angular Distributions from Fixed-in-Space Molecules

Renaud Guillemin
University of Nevada, Las Vegas

Oliver Hemmers
University of Nevada, Las Vegas, Oliver.Hemmers@unlv.edu

Dennis W. Lindle
University of Nevada, Las Vegas, lindle@unlv.nevada.edu

E. Shigemasa
Institute for Molecular Science, Japan

K. Le Guen
Université Paris-Sud

Nondipolar Electron Angular Distributions from Fixed-in-Space Molecules

R. Guillemin,[1,*] O. Hemmers,[1] D. W. Lindle,[1] E. Shigemasa,[2] K. Le Guen,[3,4] D. Ceolin,[3,4] C. Miron,[3,4] N. Leclercq,[3,4] P. Morin,[3,4] M. Simon,[3,4] and P. W. Langhoff[5]

[1]*Department of Chemistry, University of Nevada, Las Vegas, Nevada 89154-4003*
[2]*UVSOR, Institute for Molecular Science, Myodaiji, Okazaki 444-8585, Japan*
[3]*LURE, Université Paris-Sud, 91898 ORSAY Cedex, France*
[4]*CEA/DRECAM/SPAM, CEN Saclay, 91191 Gif/Yvette Cedex, France*
[5]*San Diego Supercomputer Center, University of California, La Jolla, California 92093-0505*

(Received 30 March 2002; published 26 June 2002)

The first indication of nondipole effects in the azimuthal dependence of photoelectron angular distributions emitted from fixed-in-space molecules is demonstrated in N_2. Comparison of the results with angular distributions observed for randomly oriented molecules and theoretical derivations for the nondipole correction first order in photon momentum suggests that higher orders will be needed to describe distributions measured in the molecular frame.

DOI: 10.1103/PhysRevLett.89.033002 PACS numbers: 33.60.Fy, 33.80.Eh

The understanding of interactions between light and matter has long been based on the uniform-electric-field approximation in which one assumes negligible spatial variation of the electric field over the dimensions of the absorbing charge distribution. In this so-called electric dipole approximation (DA), effects from all higher orders, such as electric-quadrupole and magnetic-dipole interactions, are neglected. An excellent probe for the interaction between light and matter is the experimental study of photoemission from atoms and molecules. In conventional gas-phase studies, owing to random orientations of the molecules, the photoelectron angular distribution is limited by angular momentum and parity conservation, within limits of the DA, to [1]

$$\frac{d\sigma(\hat{k}_e;\hbar\omega)}{d\Omega_{\hat{k}_e}} = \frac{\sigma(\hbar\omega)}{4\pi}[1 + \beta(\hbar\omega)P_2(\cos\theta_e)], \quad (1)$$

where $\hat{k}_e = (\theta_e, \phi_e)$ is the laboratory-frame direction of electron ejection, θ_e and ϕ_e are the polar angle and the azimuthal angle, respectively, and β is the anisotropy parameter completely describing the angular distribution of the photoelectrons. Although Eq. (1) is currently used to describe photoelectron emission in most angle-resolved experiments, the information provided is limited by the averaging over all possible molecular orientations. It is posfsible to access more-detailed information on photoemission dynamics and provide more-stringent tests of theory by measuring electron angular distributions from molecules in the gas phase effectively fixed in space by means of coincidence techniques [2]. In pioneering studies, Shigemasa and co-workers [3] have measured the angular distributions of photoelectrons emitted from fixed-in-space molecules in the gas phase and determined concomitant dipole matrix elements and phase-shift differences.

It is commonly known that the DA breaks down for atoms at high photon energy (>2 keV) when the wavelength becomes comparable to or smaller than the spatial extent of the electronic shells of the atom. The first experimental observations of deviations from the DA [4] were followed by intensive theoretical efforts [5–7], leading to equivalent formulations for the differential cross section including first-order nondipole corrections. Using the parametrization of Cooper [7], for 100% linearly polarized light, the differential cross section for a randomly oriented target is given, in the first order of nondipole correction, by

$$\frac{d\sigma(\hat{k}_e;\hbar\omega)}{d\Omega_{\hat{k}_e}} = \frac{\sigma(\hbar\omega)}{4\pi}\{[1 + \beta(\hbar\omega)P_2(\cos\theta_e)] + [\delta(\hbar\omega) + \gamma(\hbar\omega)\cos^2\theta_e] \times \sin\theta_e\cos\phi_e\}, \quad (2)$$

where the first-order nondipolar angular-distribution parameters $\delta(\hbar\omega)$ and $\gamma(\hbar\omega)$ result from $E_1 \otimes (E_2, M_1)$ terms in the description of photon momentum. The differential cross section now depends on the angle ϕ_e relative to the photon propagation. It has been shown recently that deviations from the DA occur in atomic gases below 1 keV [8] and in molecules at even lower photon energies, just above core ionization thresholds (<500 eV). Large deviations from the DA observed in the angular distributions of $1s$ photoelectrons of N_2 [9] suggest a potentially universal nondipole behavior in molecular photoionization above K-shell ionization thresholds. These new observations call for a review of the common dipole description.

The first theoretical development providing the differential cross section for fixed-in-space molecules including first-order nondipole corrections has been obtained recently [10]. The body-frame differential cross section can be written as a simple sum,

$$\frac{d\sigma(\hat{k}_b;\hbar\omega)}{d\Omega_{\hat{k}_b}} = \frac{2\pi e^2}{m^2 c\omega}\{\mathcal{D} + \mathcal{Q}\}, \quad (3)$$

where $\hat{k}_b = (\theta_b, \phi_b)$ is the body-frame direction of electron ejection, $\mathcal{D}$ being the dipole term and $\mathcal{Q}$ its

first-order nondipole correction. $\mathcal{Q}$ includes nondipole transition moments and depends on *both* polar and azimuthal angles. Averaging this expression over all possible molecular orientations has been shown to provide good agreement with data obtained for randomly oriented N_2 molecules [9]. In the present Letter, we report the first experimental observation of deviations from the DA in the angular distributions of photoelectrons emitted from fixed-in-space molecules ($1s$ from N_2) at relatively low photon energy (660 eV). Comparison is made with the recently developed theoretical formula in Eq. (3).

The experiment was performed at Laboratoire pour l'Utilisation du Rayonnement Electromagnétique on the bending-magnet SA22 beam line of the SuperACO storage ring which covers the 100–900 eV photon-energy range. The experimental setup has been described elsewhere [11] and successfully used to measure angular distributions of Auger electrons from fixed-in-space molecules [12]. Briefly, the incoming light is focused on a sample of gas-phase molecules. The emitted electrons are angle and energy analyzed with a double-toroidal analyzer equipped with a position-sensitive detector [13]. The design of this analyzer allows us to detect electrons emitted at 54.7° around the analyzer axis. Thus, when the analyzer axis is superimposed with the polarization axis of the ionizing radiation, the dipole angular dependence for randomly oriented molecules vanishes because the second Legendre polynomial in Eq. (3) vanishes for the so-called magic angle $\theta_e = \theta_m = 54.7°$. The measured angular distribution is then a function of the azimuthal angle ϕ_e relative to the photon propagation, θ_e being fixed, and only nondipole terms contribute to the angular dependence.

Figure 1 shows the azimuthal angular dependence of N $1s$ photoelectrons at 660 eV photon energy for randomly oriented N_2 molecules, i.e., electrons measured without coincidence with an ion. The anisotropic angular pattern shows directly the deviation from the DA in Eq. (1). The electrons are preferentially emitted in the forward direction along the photon-propagation axis. Equation (3) is valid only for 100% linearly polarized light and some corrections must be applied for data taken at beam line SA22. Shaw *et al.* [14] proposed a general equation taking into account the degree of linear polarization $\mathcal{P}$ and the tilt angle ψ between the polarization axis and the laboratory frame [Eq. (7) in Ref. [14]]. In our experimental geometry, electrons are detected at the magic angle $\theta_m = 54.7°$, and the differential cross section becomes

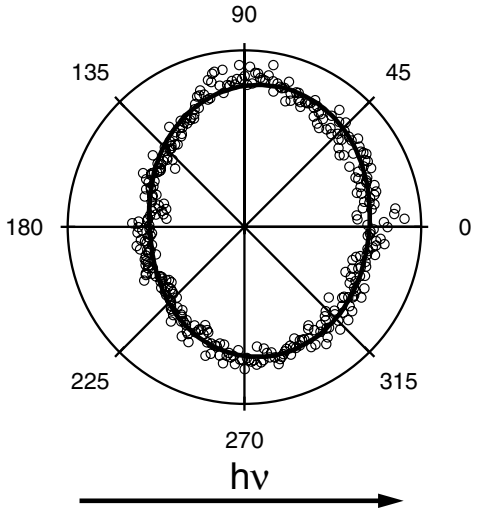

FIG. 1. Azimuthal dependence of the angular distribution for N $1s$ photoelectrons emitted from randomly oriented molecules at 660 eV photon energy (open circles) and fit obtained with Eq. (4) (solid curve). The photon propagation direction corresponds to the 180° → 0° axis.

$$\left(\frac{d\sigma(\hat{k}_e;\hbar\omega)}{d\Omega_{\hat{k}_e}}\right)(\mathcal{P},\psi) = \frac{\sigma(\hbar\omega)}{4\pi}\Big\{1 + \Big[\delta(\hbar\omega) + \frac{\gamma(\hbar\omega)}{12}(\mathcal{P}\cos2\psi + 3)\Big]\sqrt{\frac{2}{3}}\cos\phi_e + \frac{\beta(\hbar\omega)}{4}(\mathcal{P}\cos2\psi - 1)\cos2\phi_e + \frac{\gamma(\hbar\omega)}{12}(\mathcal{P}\cos2\psi - 1)\sqrt{\frac{2}{3}}\cos3\phi_e - \frac{\sqrt{2}\,\beta(\hbar\omega)}{2}\mathcal{P}\sin2\psi\sin\phi_e - \frac{\gamma(\hbar\omega)}{3\sqrt{3}}\mathcal{P}\sin2\psi\sin2\phi_e\Big\}. \quad (4)$$

This expression depends now on the dipole anisotropy parameter $\beta(\hbar\omega)$. At this energy, the β parameter has been measured to be 2 [15]. Equation (4) can be used to extract the nondipole parameters from the measured angular distribution with a least-squares fitting procedure. The results, calibrated using C $1s$ Auger emission from CO, are $\zeta = 3\delta + \gamma = 0.53 \pm 0.05$, $\delta = 0$, $\mathcal{P} = 0.85 \pm 0.03$, and $\psi = 1° \pm 0.1$. The positive value found for γ describes the forward anisotropy along the photon-propagation axis. The same measurements also have been done at 440 and 462 eV photon energies, calibrated using xenon and krypton Auger lines, respectively, and the ζ values deduced are $\zeta = 0.56 \pm 0.02$ and $\zeta = 0.87 \pm 0.03$, in excellent agreement with previously reported values [9].

Assuming the axial-recoil approximation, the photoelectron angular distribution in the molecular frame is determined by detecting the electron in coincidence with an energetic fragment ion defining the molecular-axis orientation at the moment of photoabsorption [11]. To define this axis, we use two identical ion detectors with a small acceptance angle (±3°) placed at 0° and 90° relative to the polarization axis of the incoming light, thus selecting $\Sigma \rightarrow \Sigma$ and $\Sigma \rightarrow \Pi$ ionization channels, respectively. A

retardation voltage of +5 V was applied to both ion detectors to select only energetic fragment ions for which the axial-recoil approximation is more likely to apply. As discussed previously [11], analysis of the angular-distribution data requires accurate calibration. Known electron angular distributions from rare gases are generally used for this purpose. In this work, a supplementary difficulty arose; the nondipole parameters $\delta(\hbar\omega)$ and $\gamma(\hbar\omega)$ of the calibration gas have to be known accurately. The angular distributions obtained in this work have been measured at 660 eV photon energy and calibrated using the angular distribution of C *KVV* Auger electrons from CO (*K*-shell hole, valence shell electrons). At this energy, N 1*s* photoelectrons from N_2 have the same kinetic energy as the C 1*s* Auger electrons of CO, and the energy is sufficiently above the C 1*s* threshold to assume validity of a two-step-decay model, ensuring the Auger-electron angular distribution is unaffected by first-order nondipole influences [16]. The main result of this work is shown in Fig. 2, which depicts the azimuthal angular distributions of photoelectrons emitted from fixed-in-space N_2 molecules at 660 eV photon energy for both parallel (Fig. 2a) and perpendicular (Fig. 2b) molecular orientations relative to the polarization vector. The data have been symmetrically summed point to point with respect to the horizontal plane containing the photon propagation and polarization vectors in order to increase statistics and to eliminate a slight anisotropy introduced by the tilt angle ψ. Both angular distributions, (Figs. 2a and 2b), show the forward-directed effect characterizing the first-order nondipole influence on the phototelectron angular distributions. Furthermore, the two molecular orientations lead to different angular distributions, implying that different transition moments and related phase shifts contribute in each case. For theoretical comparison, the expressions obtained by Langhoff *et al.* [10] for all possible molecular orientations (θ_R and ϕ_R in Ref. [10]) can be simplified for our experimental geometry. For parallel transitions, $\Sigma \rightarrow \Sigma$, $\theta_R = \phi_R = 0$, and we obtain

$$\begin{aligned} \mathcal{D}^{\Sigma} &= (\mu_1^{(0)})^2 |\hat{\Theta}_{\mathcal{D}}^{(0)}(\theta_b)|^2, \\ \mathcal{Q}^{\Sigma} &= 4\mu_1^{(0)}\mu_2^{(1)} \cos\phi_b \, \mathrm{Re}\{\hat{\Theta}_{\mathcal{D}}^{(0)}(\theta_b)\hat{\Theta}_{Q}^{(1)}(\theta_b)^*\}. \end{aligned} \tag{5}$$

For perpendicular transitions, $\Sigma \rightarrow \Pi$, $\theta_R = \phi_R = \pi/2$, and we obtain

$$\begin{aligned} \mathcal{D}^{\Pi} &= 2(\mu_1^{(1)})^2 \cos^2\phi_b |\hat{\Theta}_{\mathcal{D}}^{(1)}(\theta_b)|^2, \\ \mathcal{Q}^{\Pi} &= -8\sqrt{2}\,\mu_1^{(1)}\mu_2^{(2)} \cos^2\phi_b \sin\phi_b \, \mathrm{Re}\{\hat{\Theta}_{\mathcal{D}}^{(1)}(\theta_b)\hat{\Theta}_{Q}^{(2)}(\theta_b)^*\}. \end{aligned} \tag{6}$$

The coefficients $\mu_\kappa^{(\lambda_\kappa)}$ are body-frame continuum transition moments of λ_κ symmetry and $\hat{\Theta}_\kappa^{(\lambda_\kappa)}$ are corresponding angular amplitudes.

The analysis of the pattern in Fig. 2b is rather complicated because each point of the distribution is a combination of two angles θ_b and ϕ_b in the body frame, necessitating knowledge of the angular amplitudes $\hat{\Theta}_\kappa^{|(\lambda_\kappa)|}(\theta_b)$, via *ab initio* calculations. However, for $\Sigma \rightarrow \Sigma$ transitions, a straightforward analysis of the distribution (Fig. 2a) can be made because the laboratory and the body frame are superimposed. For partial linear polarization within the elliptic approximation and using Eqs. (5) and (6), we have for $\Sigma \rightarrow \Sigma$ transitions

$$\frac{d\sigma(\hat{k}_b;\hbar\omega)}{d\Omega_{\hat{k}_b}} \propto \frac{1+\mathcal{P}}{2}(\mathcal{D}^{\Sigma} + \mathcal{Q}^{\Sigma}) + \frac{1-\mathcal{P}}{2}(\mathcal{D}_y^{\Sigma}), \tag{7}$$

where $\mathcal{D}^{\Sigma}$ and $\mathcal{Q}^{\Sigma}$ are given by Eq. (5) and $\mathcal{D}_y^{\Sigma} = 2(\mu_1^{(1)})^2 \sin^2\phi_b |\hat{\Theta}_1^{(1)}(\theta_b)|^2$ gives the correction for radiation polarized in the laboratory-frame y direction.

Figure 3 replots the angular-distributions data in Fig. 2a and includes curves obtained by a least-squares fitting procedure using Eq. (5) for 100% linear polarization (dashed curve) and Eq. (7) for partial linear polarization (solid curve). The latter curve shows the influence of nonperfect polarization introduces structures in the distribution due to

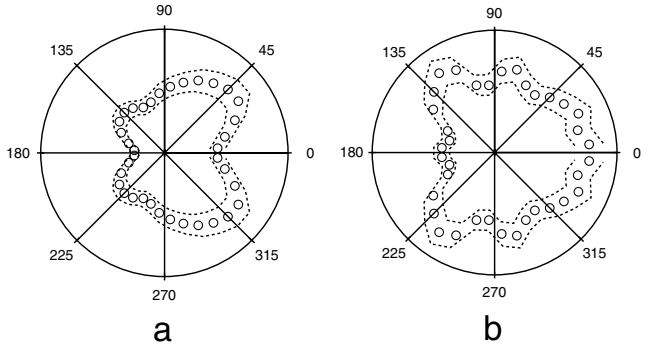

FIG. 2. Photoelectron angular distributions measured for parallel (a) and perpendicular (b) molecular orientations at 660 eV photon energy. The dashed lines represent the statistical error. In (a) the molecular axis points out of the paper, while in (b) the molecular axis is aligned along the 90°–270° axis.

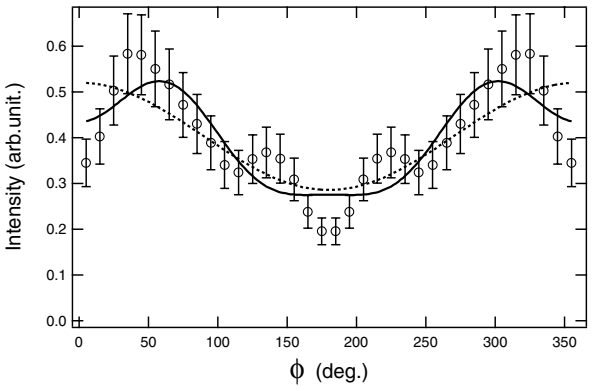

FIG. 3. Comparison between the angular distribution measured for parallel transitions (data points with statistical error bars) and fits obtained using Eq. (5) with $P = 1.0$ (dashed curve) and Eq. (7) with $P = 0.85$ (solid curve).

the $\sin^2\phi_b$ term in Eq. (7), providing some improvement in the agreement with the data. While forward/backward anisotropy is reasonably reproduced, the $\pi/4$ oscillations (peaks at 45°, 135°, 225°, and 315°) present in the measured angular distribution are absent in the fitted curves. Despite the influence of nonperfect linear polarization, it is clear higher-order terms than those included in Eq. (7) are needed to describe the observed structures in the azimuthal dependence. In light of this observation, we believe nondipole terms accounting for higher orders in photon momentum (at least second order) will have to be included to reproduce the azimuthal dependence measured for nondipolar angular distributions of photoelectrons from fixed-in-space molecules. The influence of second-order effects has already been observed in the 100-1200 eV photon energy range on neon valence photoelectrons [17]. Unlike first-order, second-order-nondipole corrections involve interference terms between electric-dipole and higher-order components but also pure-electric-quadrupole interactions. At this level approximation for the photon momentum, the total photoionization cross section $\sigma(\hbar\omega)$ is affected directly, not just the photoelectron angular distribution. Evidence of a significant influence from second-order components at relatively low photon energies would have important consequences to our understanding of molecular photoabsorption processes. Nowadays, experimental techniques are available that resolve continuum electron wave functions in the molecular frame in order to determine matrix elements and phase-shift differences as a further step towards the so-called "complete experiment." The present results call for a renewal of the theory accompanying the latest experimental developments in molecular physics.

In summary, we measured nondipole-influenced angular distributions of photoelectrons emitted from fixed-in-space N_2 molecules at 660 eV photon energy. Comparing the distribution obtained for $\Sigma \rightarrow \Sigma$ transitions with theoretical expressions including first-order-nondipole corrections, we have shown higher orders need to be included as well. Further investigation is required in order to clarify the origin(s) of the nondipole behavior observed above molecular $1s$ ionization thresholds.

This work was partly funded by National Science Foundation Award No. PHY-9876996. We are grateful for the hospitality of the SuperACO staff.

*Electronic address: RGuillemin@lbl.gov

[1] J. Cooper and R. N. Zare, J. Chem. Phys. **48**, 942 (1968).
[2] A. V. Golovin, N. A. Cherepkov, and V. V. Kuznetsov, Z. Phys. D **24**, 371 (1992).
[3] E. Shigemasa, J. Adachi, M. Oura, and A. Yagishita, Phys. Rev. Lett. **74**, 359 (1995); E. Shigemasa, J. Adachi, K. Soejima, N. Watanabe, A. Yagishita, and N. A. Cherepkov, Phys. Rev. Lett. **80**, 1622 (1998).
[4] M. O. Krause, Phys. Rev. **177**, 151 (1969); F. J. Wuilleumier and M. O. Krause, Phys. Rev. A **10**, 242 (1974).
[5] R. H. Pratt, A. Ron, and H. K. Tseng, Rev. Mod. Phys. **45**, 273 (1973).
[6] A. Bechler and R. H. Pratt, Phys. Rev. A **39**, 1774 (1989).
[7] J. W. Cooper, Phys. Rev. A **42**, 6942 (1990).
[8] D. W. Lindle and O. Hemmers, J. Electron Spectrosc. Relat. Phenom. **100**, 297 (1999).
[9] O. Hemmers, H. Wang, P. Focke, I. A. Sellin, D. W. Lindle, J. C. Arce, J. A. Sheehy, and P. W. Langhoff, Phys. Rev. Lett. **87**, 273003 (2001).
[10] P. Langhoff, J. C. Arce, J. A. Sheehy, O. Hemmers, H. Wang, P. Focke, I. A. Sellin, and D. W. Lindle, J. Electron Spectrosc. Relat. Phenom. **114–116**, 23 (2001).
[11] R. Guillemin, E. Shigemasa, and K. Le Guen, D. Ceolin, C. Miron, N. Leclercq, K. Ueda, P. Morin, and M. Simon, Rev. Sci. Instrum. **71**, 4387 (2000).
[12] R. Guillemin, E. Shigemasa, and K. Le Guen, D. Ceolin, C. Miron, N. Leclercq, P. Morin, and M. Simon, Phys. Rev. Lett. **87**, 203001 (2001).
[13] C. Miron, M. Simon, N. Leclercq, and P. Morin, Rev. Sci. Instrum. **68**, 3728 (1997).
[14] P. S. Shaw, U. Arp, and S. H. Southworth, Phys. Rev. A **54**, 1463 (1996).
[15] D. W. Lindle, P. H. Kobrin, C. M. Truesdale, T. A. Ferret, P. A. Heimann, U. Becker, H. G. Kerkhoff, and D. A. Shirley, J. Chem. Phys. **81**, 5375 (1984).
[16] N. M. Kabachnik and I. P. Sazhina, J. Phys. B **29**, L515 (1996).
[17] A. Derevianko, O. Hemmers, S. Oblad, P. Glans, H. Wang, S. B. Whitfield, R. Wehlitz, I. A. Sellin, W. R. Johnson, and D. W. Lindle, Phys. Rev. Lett. **84**, 2116 (2000).